

Effective-field theory analysis of the $\tau^- \rightarrow (K\pi)^- \nu_\tau$ decays

Javier Rendón*[†]

Cinvestav, Apdo. Postal 14-740, 07000 Ciudad de México, México

E-mail: jrendon@fis.cinvestav.mx

In this work we consider the most general analysis of $\tau \rightarrow (K\pi)^- \nu_\tau$ decays within an effective field theory description of heavy new physics (NP) including SM operators up to dimension six with massless neutrinos. All hadron form factors are built exploiting chiral symmetry, dispersion relations and (lattice) data. Within this framework we:

- i) confirm that it is impossible to understand the BaBar anomaly in the CP asymmetry measurement (we find an upper bound for the NP contribution slightly larger than in Phys. Rev. Lett. 120 (2018) no.14, 141803, but still irrelevant compared to the experimental uncertainty by four orders of magnitude approximately);
- ii) first show that the anomalous bump measured in the Belle experiment for the $K_S\pi^-$ invariant mass distribution at low energies is also impossible to understand in the presence of heavy NP;
- iii) first bind the heavy NP effective couplings using $\tau^- \rightarrow (K\pi)^- \nu_\tau$ decays and show that they are competitive with those found in hyperon semileptonic decays (but clearly not with those obtained for non-standard scalar interactions in Kaon (semi)leptonic decays).

Finally to have a good control of potential new physics effects, we study carefully the SM contribution, namely, we compare the SM predictions with possible deviations caused by NP in three different observables: a couple of Dalitz plot distributions, in the forward-backward asymmetry and in the di-meson invariant mass distribution.

7th Annual Conference on Large Hadron Collider Physics - LHCP2019

20-25 May, 2019

Puebla, Mexico

*Speaker.

[†]I thank conacyt for my PhD scholarship and also my advisor P.R for the project 250628 (Ciencia Básica).

1. Introduction

This work is based in an article that we have published recently, for more details see ref. [1]. In this article we focus on the $\tau^- \rightarrow (K\pi)^- \nu_\tau$ decays, that we study within the SM and considering the effects of heavy new physics (NP) on a number of phenomenologically interesting observables. A clear motivation for this is the BaBar anomalous measurement of the CP asymmetry in the $K_S\pi^-$ channel [2]. The CP violation present in the SM [3] is clearly insufficient to understand the baryon asymmetry of the universe [4, 5, 6] so that any hint of NP involving CP violation becomes a candidate for providing with a clue to understand the enormous matter-antimatter imbalance. With respect to this BaBar anomaly, however, the related Belle measurement [7] of a binned CP asymmetry in the same decay channel analyzing the decay angular distributions is compatible with zero, as expected in the SM with a permille level precision. On the theoretical side, Ref. [8] proved that heavy NP cannot explain this anomaly. We will also confirm this last statement.

Another motivation to do this study is that three data points at the beginning of the $K_S\pi^-$ spectra measured by Belle [9] have been excluded from the reference fits or signalled as controversial in the dedicated analyses [10, 11, 12, 13, 15, 14, 16, 17] and are at odds with the prediction [18]. To our knowledge, only Ref. [19] was able to describe these data points due to the effect on the scalar form factor of the longitudinal correction to the $K^*(892)$ propagator induced by flavor symmetry breaking¹. We will study if it is possible to explain these conflicting data points by the most general description of heavy NP contributions modifying the $\tau^- \rightarrow \bar{u}s\nu_\tau$ decays in the SM.

Finally, the third motivation to do this work is that semileptonic tau decays [20, 21, 22] have been proved competitive with the traditional semileptonic decays involving light quarks [23, 24, 25, 26, 27, 28, 29, 30, 31, 32, 33], like nuclear beta or leptonic and radiative pion decays. In this context, for the Cabibbo-suppressed sector, hyperon semileptonic decays [27, 30] cannot compete with (semi)leptonic Kaon decays [29], given the (very accurately measured) dominant branching fractions of the latter and the suppressed ones (at most at the permille level) of the former. This intuitive reasoning suggests that strangeness-changing tau decays can also give non-trivial bounds on non-standard charged current interactions, although it is not likely that a competitive level with $K_{\ell(2,3)}$ decays. The present work will make these statements precise.

In ref. [34] one can see restrictions in the effective couplings in $\tau^- \rightarrow K^- \nu_\tau$ decays which are analogous and also complementary to the ones we will make here, both in the $|\Delta S| = 1$ sector.

2. Effective theory analysis of $\tau^- \rightarrow \nu_\tau \bar{u}s$

The lepton number conserving effective Lagrangian density constructed with dimension six operators and invariant under the local $SU(3)_C \otimes SU(2)_L \otimes U(1)_Y$ SM gauge group has the following form [35, 36],

$$\mathcal{L}^{(eff)} = \mathcal{L}_{SM} + \frac{1}{\Lambda^2} \sum_i \alpha_i \mathcal{O}_i \longrightarrow \mathcal{L}_{SM} + \frac{1}{v^2} \sum_i \hat{\alpha}_i \mathcal{O}_i, \quad (2.1)$$

¹As we will recall in section 4, the scalar form factor contribution that we employ [37] was obtained as a result of analyzing strangeness-changing meson-meson scattering [38] within Chiral Perturbation Theory [39, 40] with resonances [41, 42], accounting for the leading flavor symmetry breaking.

with $\hat{\alpha}_i = (v^2/\Lambda^2)\alpha_i$ the dimensionless couplings encoding NP at a scale of some TeVs.

Upon integrating the heavy degrees of freedom out we can explicitly construct the low-scale $O(1\text{GeV})$ effective lagrangian for semi-leptonic transitions as follows [23, 24]:

$$\begin{aligned} \mathcal{L}_{cc} = & -\frac{G_F V_{us}}{\sqrt{2}}(1 + \varepsilon_L + \varepsilon_R) \left[\bar{\tau} \gamma_\mu (1 - \gamma_5) \nu_\ell \cdot \bar{u} [\gamma^\mu - (1 - 2\hat{\varepsilon}_R) \gamma^\mu \gamma_5] s \right. \\ & \left. + \bar{\tau} (1 - \gamma_5) \nu_\ell \cdot \bar{u} [\hat{\varepsilon}_s - \hat{\varepsilon}_p \gamma_5] s + 2\hat{\varepsilon}_T \bar{\tau} \sigma_{\mu\nu} (1 - \gamma_5) \nu_\ell \cdot \bar{u} \sigma^{\mu\nu} s \right] + \text{h.c.}, \end{aligned} \quad (2.2)$$

where $\hat{\varepsilon}_i = \varepsilon_i / (1 + \varepsilon_L + \varepsilon_R)$ [20] for $i = R, S, P, T$.

3. Semileptonic τ decay amplitude

In this section we calculate the decay amplitudes corresponding to the $\tau^- \rightarrow \bar{K}^0 \pi^- \nu_\tau$ and the $\tau^- \rightarrow K^- \pi^0 \nu_\tau$ decays. The first thing to note is that due to the parity of pseudoscalar mesons, only the vector, scalar and tensor currents give a non-zero contribution to the decay amplitude, as shown in the following equation^{2 3}

$$\begin{aligned} \mathcal{M} = & \mathcal{M}_V + \mathcal{M}_S + \mathcal{M}_T \\ = & \frac{G_F V_{us} \sqrt{S_{EW}}}{\sqrt{2}} (1 + \varepsilon_L + \varepsilon_R) [L_\mu H^\mu + \hat{\varepsilon}_S L H + 2\hat{\varepsilon}_T L_{\mu\nu} H^{\mu\nu}], \end{aligned} \quad (3.1)$$

where the leptonic currents have the following structure (p and p' are the momenta of the tau lepton and its neutrino, respectively),

$$\begin{aligned} L_\mu = & \bar{u}(p') \gamma_\mu (1 - \gamma_5) u(p), \\ L = & \bar{u}(p') (1 + \gamma_5) u(p), \\ L_{\mu\nu} = & \bar{u}(p') \sigma_{\mu\nu} (1 + \gamma_5) u(p), \end{aligned} \quad (3.2)$$

and the vector, scalar and tensor hadronic matrix elements for the case of the $\tau^- \rightarrow \bar{K}^0 \pi^- \nu_\tau$ decay, are defined as follows

$$H^\mu = \langle \pi^- \bar{K}^0 | \bar{s} \gamma^\mu u | 0 \rangle = Q^\mu F_+(s) + \frac{\Delta_{K\pi}}{s} q^\mu F_0(s), \quad (3.3)$$

$$H = \langle \pi^- \bar{K}^0 | \bar{s} u | 0 \rangle = F_S(s), \quad (3.4)$$

$$H^{\mu\nu} = \langle \pi^- \bar{K}^0 | \bar{s} \sigma^{\mu\nu} u | 0 \rangle = iF_T(s) (p_K^\mu p_\pi^\nu - p_\pi^\mu p_K^\nu), \quad (3.5)$$

where $q^\mu = (p_\pi + p_K)^\mu$, $Q^\mu = (p_K - p_\pi)^\mu - \frac{\Delta_{K\pi}}{s} q^\mu$, $s = q^2$, and $\Delta_{ij} = m_i^2 - m_j^2$. The hadron matrix elements H , H^μ and $H^{\mu\nu}$ were decomposed in terms of the allowed Lorentz structures, taking into

²Eq.(3.1) displays clearly that the renormalization scale dependence of the Wilson coefficients $\hat{\varepsilon}_i$ needs to be cancelled by the one of the hadron matrix elements. As it is conventional, both are defined in the \overline{MS} scheme at $\mu = 2$ GeV.

³For convenience, the short-distance electroweak correction factor S_{EW} [43, 44, 45, 46, 47, 48, 49, 50] is written as an overall constant, although it only affects the SM contribution. The error of this simplification is negligible working at leading order in the $\hat{\varepsilon}_i$ coefficients [20, 21].

account the discrete symmetries of the strong interactions, and a number of scalar functions of the invariant mass of the $K\pi$ system: the $F_S(s)$, $F_+(s)$, $F_0(s)$ and $F_T(s)$ form factors; which encode the details of the hadronization procedure.

The $\tau^- \rightarrow K^- \pi^0 \nu_\tau$ decay is completely analogous. Neglecting (tiny) isospin corrections, the only difference is given by the Clebsch-Gordan flavor symmetry factor of $\sqrt{2}$ between both decay channels, that is $\sqrt{2}F_{0,+}^{K^- \pi^0}(s) = F_{0,+}^{\bar{K}^0 \pi^-}(s)$.

From equations (3.2) one can easily see that the vector and the scalar currents are related through the Dirac equation in the following way

$$L = \frac{L_\mu q^\mu}{M_\tau}. \quad (3.6)$$

Similarly, one can find a relation between the vector and the scalar hadronic matrix elements by taking the four-divergence of equation (3.3). This yields

$$F_S(s) = \frac{\Delta_{K\pi}}{m_s - m_u} F_0(s). \quad (3.7)$$

Taking into account the previous two equations, we conclude that the scalar and vector contributions in eq.(3.1) can be treated jointly by doing the convenient replacement

$$\frac{\Delta_{K\pi}}{s} \rightarrow \frac{\Delta_{K\pi}}{s} \left[1 + \frac{s \hat{\epsilon}_s}{M_\tau(m_s - m_u)} \right]. \quad (3.8)$$

4. Hadronization of the scalar, vector and tensor currents

The form factors encode the details of the hadronization process and are extremely important to have a good control of the SM and in consequence to constrain the non-standard interactions. These are constructed exploiting chiral symmetry, dispersion relations and lattice data when needed.

The scalar and the vector form factors have been studied extensively, here we benefit from previous works for both of them. The vector form factor is taken from ref. [12] and the scalar form factor is taken from ref. [51]. Here we focus in the analysis of the tensor form factor which is the new ingredient in this work, the normalization of the tensor form factor at zero-momentum-transfer is obtained using Chiral Perturbation Theory with tensor sources [52] and Lattice data [53];

$$i \langle \pi^- \bar{K}^0 | \frac{\delta \mathcal{L}}{\delta \bar{l}_{\alpha\beta}} | 0 \rangle = \frac{\Lambda_2}{F^2} (p_K^\alpha p_0^\beta - p_0^\alpha p_K^\beta). \quad (4.1)$$

The energy-dependence of the tensor form factor $F_T(s)$ is calculated using a phase dispersive representation as it is shown in refs. [8] and [21];

$$\frac{F_T(s)}{F_T(0)} = \exp \left[\frac{s}{\pi} \int_{s_{\pi K}}^{\infty} ds' \frac{\delta_T(s')}{s'(s' - s - i\epsilon)} \right], \quad (4.2)$$

where $s_{\pi K} = (m_{\bar{K}^0} + m_{\pi^-})^2$. As in the scalar case we have included one subtraction. In this case it is clear, that lacking precise low-energy information, we cannot increase the number of subtractions of $F_T(s)$. This, in turn, implies a sizable sensitivity to the upper limit of the integral that is used

numerically (s_{cut}), which is illustrated in our figure 1, where we consider the cases $s_{cut} = M_\tau^2, 4, 9$ GeV² [21]⁴. We take the differences between these curves as an estimate of our systematic theoretical error on $F_T(s)/F_T(0)$. In the right panel of fig. 1 we show the tensor form factor phase corresponding to $\delta_T(s) = \delta_+(s)$, with $\delta_+(s)$ from the fits in table 1 of Ref. [13]. In the inelastic region, our curve plotted for $\delta_T(s)$ lies within the error band shown in figure 2 of Ref. [8]⁵.

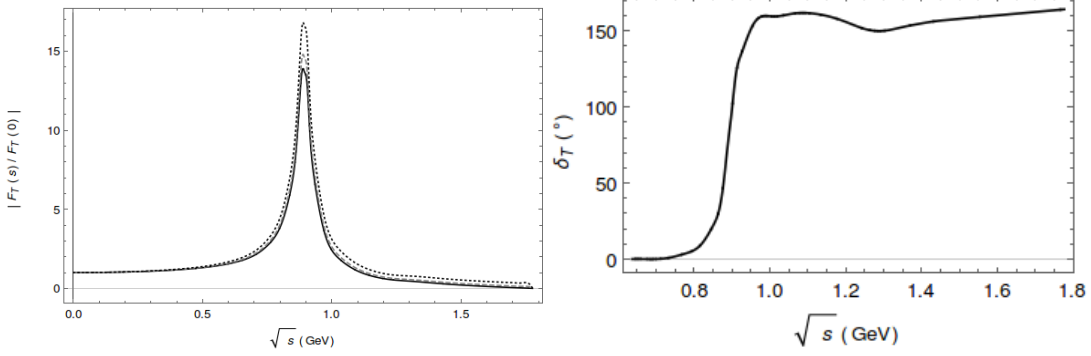


Figure 1: Modulus and phase, $|F_T(s)|$ (left) and $\delta_T(s) = \delta_+(s)$ (right), of the tensor form factor, $F_T(s)$. On the left plot, the dotted line corresponds to $s_{cut} = 9$ GeV², the dashed one to $s_{cut} = 4$ GeV², and the solid one to $s_{cut} = M_\tau^2$.

5. Decay observables

In the rest frame of the τ lepton, the doubly differential decay width for the $\tau^- \rightarrow K_S \pi^- \nu_\tau$ process is

$$\frac{d^2\Gamma}{dsdt} = \frac{1}{32(2\pi)^3 M_\tau^3} \overline{|\mathcal{M}|^2}, \quad (5.1)$$

where $\overline{|\mathcal{M}|^2}$ is given by eq. (5.3), s is the invariant mass of the $\pi^- K_S$ system taking values in the $(m_{K^0} + m_{\pi^-})^2 \leq s \leq M_\tau^2$ interval, and

$$t^\pm(s) = \frac{1}{2s} \left[2s(M_\tau^2 + m_{K^0}^2 - s) - (M_\tau^2 - s)(s + m_{\pi^-}^2 - m_{K^0}^2) \pm (M_\tau^2 - s) \sqrt{\lambda(s, m_{\pi^-}^2, m_{K^0}^2)} \right], \quad (5.2)$$

with $\lambda(x, y, z) = x^2 + y^2 + z^2 - 2xy - 2xz - 2yz$ being the usual Källén function and $t = (P_\tau - p_\pi)^2$.

5.1 Dalitz plots

The unpolarized spin-averaged squared amplitude is given as follows:

$$\overline{|\mathcal{M}|^2} = G_F^2 |V_{us}|^2 S_{EW} (1 + \varepsilon_L + \varepsilon_R)^2 (M_{0+} + M_{T+} + M_{T0} + M_{00} + M_{++} + M_{TT}). \quad (5.3)$$

In the left panel of figure 2 we show the Dalitz plot for the SM case in the (s, t) variables, which is just eq. (5.3) with $\hat{\varepsilon}_S$ and $\hat{\varepsilon}_T$ turned off.

⁴In principle, one could try to reduce this sensitivity following the strategies employed in Ref. [54], but the procedure will again be limited in this case by the absence of measurements sensitive to $F_T(s)$.

⁵Our phase is given in degrees while theirs is in radians.

When we take into account NP effects in the Dalitz plots, it is convenient to define the following observable introduced in Ref. [21]

$$\tilde{\Delta}(\hat{\epsilon}_S, \hat{\epsilon}_T) = \frac{|\overline{|\mathcal{M}(\hat{\epsilon}_S, \hat{\epsilon}_T)|^2} - \overline{|\mathcal{M}(0,0)|^2}|}{\overline{|\mathcal{M}(0,0)|^2}}, \quad (5.4)$$

which is sensitive to the relative difference between the squared matrix element in presence/absence of NP contributions (the SM case corresponds to $\mathcal{M}(0,0)$).

In the left part of figures 3 and 4 we show the corresponding plots for the values $(\hat{\epsilon}_S = -0.5, \hat{\epsilon}_T = 0)$ and $(\hat{\epsilon}_S = 0, \hat{\epsilon}_T = 0.6)$, respectively. The election of these particular values of the $\hat{\epsilon}_{S,T}$ is discussed in section 5.5.

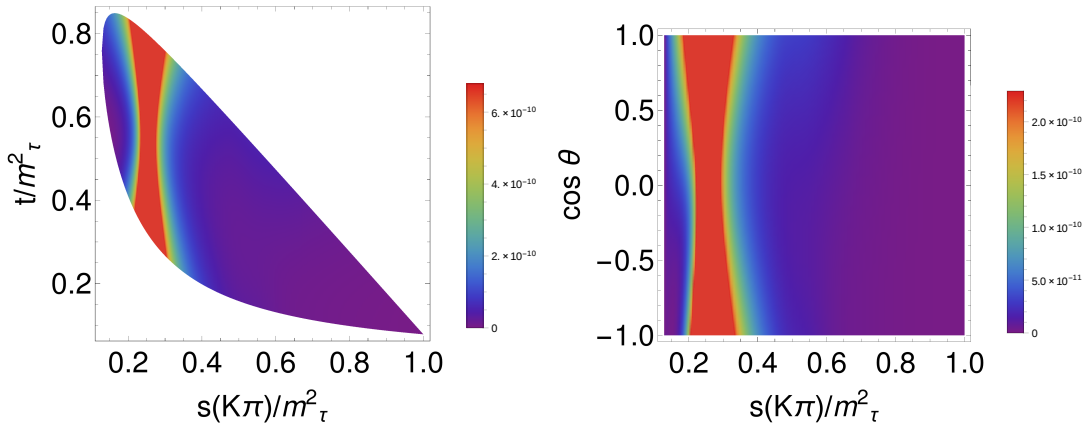


Figure 2: Dalitz plot distribution $\overline{|\mathcal{M}|^2}_{00}$ in the SM, eq. (5.3): Differential decay distribution for $\tau^- \rightarrow K_S \pi^- \nu_\tau$ in the (s, t) variables (left). The right-hand figure shows the differential decay distribution in the $(s, \cos\theta)$ variables, eq. (5.5). The Mandelstam variables, s and t , are normalized to M_τ^2 .

In the SM plots (figure 2) it is clearly appreciated that the dynamics is dominated by the $K^*(892)$ vector resonance but the effect of its excitation $K^*(1410)$ and of the dynamically generated $K_0^*(700)$ [55], of the $K_0^*(1430)$ and heavier states cannot be appreciated from the figure, although it is visible both in $F_+(s)$ and the decay spectrum [12] and in $F_0(s)$ [51], respectively. The left panel of figures 3 and 4 shows the relative modification of the squared matrix element for non-zero reasonable values of $\hat{\epsilon}_S$ and $\hat{\epsilon}_T$ in the (s, t) plane. Although large variations are seen in a couple of regions close to the border of the Dalitz plot in figure 3 (left), these correspond to zones with very suppressed probability, as can be seen in figure 2 (left). On the contrary, the regions with larger probability have a small relative change, according to figure 3 (left). In figure 4 (left) the region with the most noticeable change (though still smaller than those seen in figure 3) is located very close to the s minimum of the Dalitz plot, which has very small probability density in figure 2 (left). This region quite overlaps with one of the two mentioned for the fig. 3 left plot. Because of this feature, observing a deviation from the SM result in this region could be due to both tensor and non-standard scalar interactions. On the contrary, a deviation in the region of small t values would be signalling spin-zero NP contribution. In any case, changes are very small in the region most

densely populated by measured events in both left plots of figs. 3 and 4. Due to this, we conclude that it will be extremely challenging to identify NP contributions in the (s, t) Dalitz plot even with the large data samples accumulated by the end of operation of Belle-II [56].

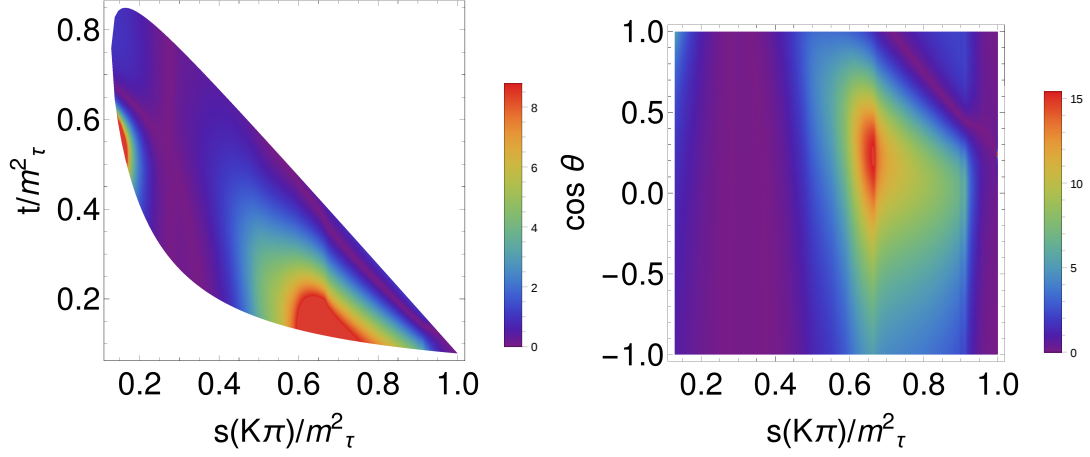


Figure 3: Dalitz plot distribution $\tilde{\Delta}(\hat{\epsilon}_S, \hat{\epsilon}_T)$, eq. (5.4), in the $\tau^- \rightarrow K_S \pi^- \nu_\tau$ decays: left-hand side corresponds to eq. (5.3) and the right-hand side corresponds to the differential decay distribution in the $(s, \cos\theta)$ variables, eq. (5.5), both with $(\hat{\epsilon}_S = -0.5, \hat{\epsilon}_T = 0)$. The Mandelstam variables, s and t , are normalized to M_τ^2 .

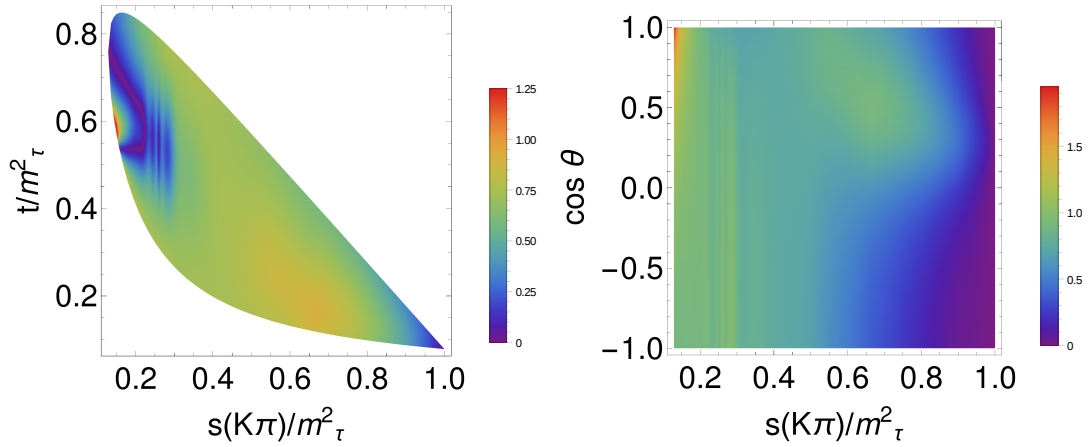


Figure 4: Dalitz plot distribution $\tilde{\Delta}(\hat{\epsilon}_S, \hat{\epsilon}_T)$, eq. (5.4), in the $\tau^- \rightarrow K_S \pi^- \nu_\tau$ decays: left-hand side corresponds to eq. (5.3) and the right-hand side corresponds to the differential decay distribution in the $(s, \cos\theta)$ variables, eq. (5.5), both with $(\hat{\epsilon}_S = 0, \hat{\epsilon}_T = 0.6)$. The Mandelstam variables, s and t , are normalized to M_τ^2 .

5.2 Angular distribution

In this section we are going to study the angular dependence of the decay distribution. It is convenient to work in the rest frame of the hadronic system, in which we have $\vec{p}_\pi + \vec{p}_K = \vec{p}_\tau - \vec{p}_\nu = \vec{0}$, consequently the tau lepton and the pion energies are given by $E_\tau = (s + M_\tau^2)/(2\sqrt{s})$

and $E_\pi = (s + m_\pi^2 - m_K^2)/(2\sqrt{s})$.

We will study the decay distribution in terms of the $(s, \cos\theta)$ variables, where θ is the angle between the three-momenta of the pion and the three-momenta of the tau lepton, this angle is related to the invariant t variable by $t = M_\tau^2 + m_\pi^2 - 2E_\tau E_\pi + 2|\vec{p}_\pi||\vec{p}_\tau|\cos\theta$, where $|\vec{p}_\pi| = \sqrt{E_\pi^2 - m_\pi^2}$ and $|\vec{p}_\tau| = \sqrt{E_\tau^2 - M_\tau^2}$ ⁶.

Changing variables to $(s, \cos\theta)$ in eq. (5.1) we obtain the following:

$$\begin{aligned} \frac{d^2\Gamma}{d\sqrt{s}d\cos\theta} &= \frac{G_F^2 |V_{us}|^2 S_{EW}}{128\pi^3 M_\tau} (1 + \varepsilon_L + \varepsilon_R)^2 \left(\frac{M_\tau^2}{s} - 1\right)^2 |\vec{p}_{\pi^-}| \left\{ \Delta_{\pi K}^2 |F_0(s)|^2 \right. \\ &\quad \times \left(1 + \frac{s\hat{\varepsilon}_S}{M_\tau(m_s - m_u)}\right)^2 + 16|\vec{p}_{\pi^-}|^2 s^2 \left| -\frac{F_+(s)}{2M_\tau} + \hat{\varepsilon}_T F_T(s) \right|^2 \\ &\quad + 4|\vec{p}_{\pi^-}|^2 s \left(1 - \frac{s}{M_\tau^2}\right) \cos^2\theta [|F_+(s)|^2 - 4s\hat{\varepsilon}_T^2 |F_T(s)|^2] + 4\Delta_{\pi K} |\vec{p}_{\pi^-}| \sqrt{s} \cos\theta \\ &\quad \left. \times \left(1 + \frac{s\hat{\varepsilon}_S}{M_\tau(m_s - m_u)}\right) \left[-\text{Re}[F_0(s)F_+^*(s)] + \frac{2s\hat{\varepsilon}_T}{M_\tau} \text{Re}[F_T(s)F_0^*(s)] \right] \right\}. \end{aligned} \quad (5.5)$$

The Dalitz plots for the $(s, \cos\theta)$ variables are shown on the right panels of figures 2, 3 and 4 (in these last two the observable $\tilde{\Delta}(\hat{\varepsilon}_S, \hat{\varepsilon}_T)$ is plotted). On figure 2 we plot the SM case, and in figures 3 and 4 we show Dalitz plots for the values $(\hat{\varepsilon}_S = -0.5, \hat{\varepsilon}_T = 0)$ and $(\hat{\varepsilon}_S = 0, \hat{\varepsilon}_T = 0.6)$, respectively. The SM plot gives equivalent information in the $(s, \cos\theta)$ variables as the one seen in the (s, t) variables (right versus left plot of figure 2). Comparing both panels of figs. 3 one can see that one of the enhanced regions in the (s, t) plot (the one at very low s values) is washed away in the $(s, \cos\theta)$ diagram, while the other is slightly further enhanced in a limited region ($0 \leq \cos\theta \leq 0.5$). The comparison of the left and right plots of figure 4 shows that the enhanced area for large t values is a bit more prominent in the $(s, \cos\theta)$ distribution (for nearly maximal $\cos\theta$) although again it will be very hard to disentangle these possible deviations from the SM patterns in near future data. Assuming approximate lepton universality, using the bounds from Ref. [29] (obtained analyzing Kaon (semi)leptonic decays) $\hat{\varepsilon}_S \sim -8 \times 10^{-4}$, $\hat{\varepsilon}_T \sim 6 \times 10^{-3}$ (maximum allowed absolute values at one standard deviation) minimizes the deviations from the SM to unobservable level both in the (s, t) and $(s, \cos\theta)$ Dalitz plots.

5.3 Decay rate

Integrating eq. (5.1) upon the t variable we obtain the invariant mass distribution as follows

$$\begin{aligned} \frac{d\Gamma}{ds} &= \frac{G_F^2 |V_{us}|^2 M_\tau^3 S_{EW}}{384\pi^3 s} (1 + \varepsilon_L + \varepsilon_R)^2 \left(1 - \frac{s}{M_\tau^2}\right)^2 \lambda^{1/2}(s, m_\pi^2, m_K^2) \\ &\quad \times [X_{VA} + \hat{\varepsilon}_S X_S + \hat{\varepsilon}_T X_T + \hat{\varepsilon}_S^2 X_{S^2} + \hat{\varepsilon}_T^2 X_{T^2}], \end{aligned} \quad (5.6)$$

⁶The tau lifetime and decay width (τ_τ and Γ_τ , respectively) are defined in the τ rest frame. Consequently, their values are boosted in the reference frame considered in this subsection.

where

$$X_{VA} = \frac{1}{2s^2} \left[3|F_0(s)|^2 \Delta_{K\pi}^2 + |F_+(s)|^2 \left(1 + \frac{2s}{M_\tau^2} \right) \lambda(s, m_\pi^2, m_K^2) \right], \quad (5.7a)$$

$$X_S = \frac{3}{sM_\tau} |F_0(s)|^2 \frac{\Delta_{K\pi}^2}{m_s - m_d}, \quad (5.7b)$$

$$X_T = \frac{6}{sM_\tau} \text{Re}[F_T(s)F_+^*(s)] \lambda(s, m_\pi^2, m_K^2), \quad (5.7c)$$

$$X_{S^2} = \frac{3}{2M_\tau^2} |F_0(s)|^2 \frac{\Delta_{K\pi}^2}{(m_s - m_u)^2}, \quad (5.7d)$$

$$X_{T^2} = \frac{4}{s} |F_T(s)|^2 \left(1 + \frac{s}{2M_\tau^2} \right) \lambda(s, m_\pi^2, m_K^2). \quad (5.7e)$$

Note from the previous equations that the only possible source of CP violation coming from the hadronic part is due to the Vector-Tensor interference, we will comment about this in section 6.

In figure 5, we plot the invariant mass distribution of the $K\pi$ system for $\tau^- \rightarrow K_S \pi^- \nu_\tau$ decays for the SM case and for $(\hat{\epsilon}_S = -0.5, \hat{\epsilon}_T = 0)$ and $(\hat{\epsilon}_S = 0, \hat{\epsilon}_T = 0.6)$ which would be realistic values for these couplings, according to their impact on the decay width. Despite the logarithmic scale of the plot, the deviations from the SM curve shown in figure 5 are too large when they are confronted with the Belle measurements of this spectrum, as we will see in the fits of section 5.5. This will allow us to set better bounds on $\hat{\epsilon}_{S,T}$ than those used in this subsection.

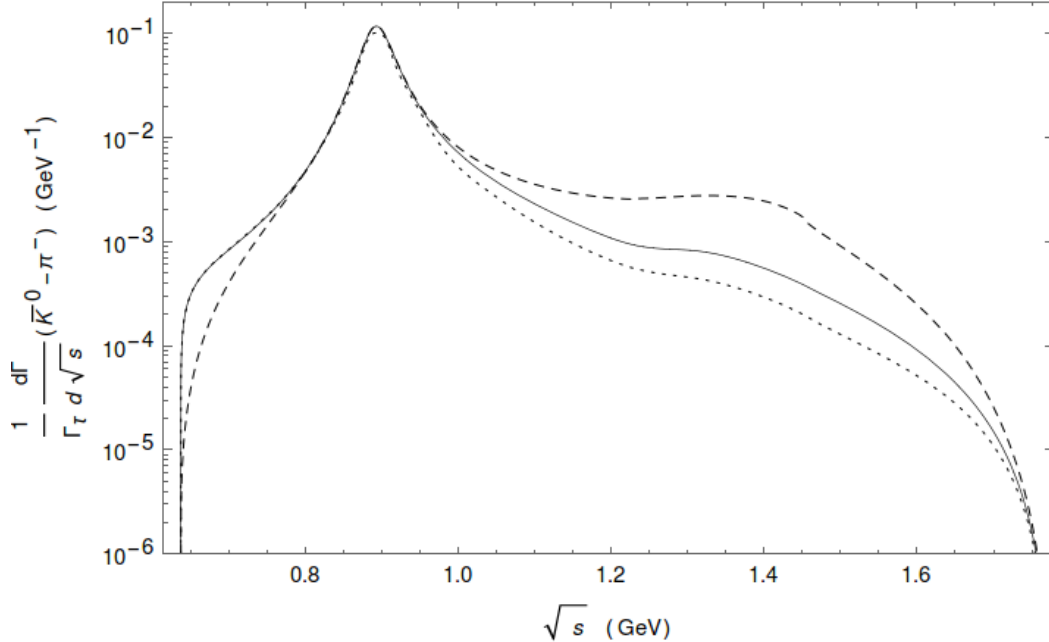


Figure 5: The $\bar{K}^0 \pi^-$ hadronic invariant mass distribution for the SM (solid line) and $\hat{\epsilon}_S = -0.5$, $\hat{\epsilon}_T = 0$ (dashed line) and $\hat{\epsilon}_S = 0$, $\hat{\epsilon}_T = 0.6$ (dotted line). The decay distributions are normalized to the tau decay width.

5.4 Forward-backward asymmetry

The forward-backward asymmetry is defined in analogy to the di-pion mode [21]

$$\mathcal{A}_{K\pi}(s) = \frac{\int_0^1 d\cos\theta \frac{d^2\Gamma}{dsd\cos\theta} - \int_{-1}^0 d\cos\theta \frac{d^2\Gamma}{dsd\cos\theta}}{\int_0^1 d\cos\theta \frac{d^2\Gamma}{dsd\cos\theta} + \int_{-1}^0 d\cos\theta \frac{d^2\Gamma}{dsd\cos\theta}}. \quad (5.8)$$

Substituting eq. (5.5) into eq. (5.8) and integrating upon the $\cos\theta$ variable we obtain its analytical expression⁷

$$\begin{aligned} \mathcal{A}_{K\pi} = & \frac{3\sqrt{\lambda(s, m_\pi^2, m_K^2)}}{2s^2[X_{VA} + \hat{\epsilon}_S X_S + \hat{\epsilon}_T X_T + \hat{\epsilon}_S^2 X_{S^2} + \hat{\epsilon}_T^2 X_{T^2}]} \left(1 + \frac{s\hat{\epsilon}_S}{M_\tau(m_s - m_u)} \right) \Delta_{\pi K} \\ & \times \left[-\text{Re}[F_0(s)F_+^*(s)] + \frac{2s\hat{\epsilon}_T}{M_\tau} \text{Re}[F_T(s)F_0^*(s)] \right]. \end{aligned} \quad (5.9)$$

The forward-backward asymmetry for the case in which $\epsilon_R = \epsilon_L = \hat{\epsilon}_S = \hat{\epsilon}_T = 0$, corresponding to the SM, is plotted in figure 6. It should not be difficult to measure a non-zero forward-backward asymmetry around $\sqrt{s} \sim 0.6$ GeV. Above the onset of inelasticities ($\sqrt{s} \gtrsim 1.05$ GeV) the theory uncertainty starts to increase up to the kinematical upper limit of \sqrt{s} . It was already emphasized long ago that a measurement of the forward-backward asymmetry in this decay channel would be crucial in improving our knowledge of both vector and scalar form factors [57]⁸.

In figure 7, we plot $\mathcal{A}_{K\pi}$ for the values ($\hat{\epsilon}_S = -0.5, \hat{\epsilon}_T = 0$) and ($\hat{\epsilon}_S = 0, \hat{\epsilon}_T = 0.6$), and we compare those plots with the SM case. For quite large $\hat{\epsilon}_T$ values some difference is appreciated for the tensor case; otherwise it may not be possible to disentangle it from the standard contribution. On the contrary, for non-standard scalar interaction, $A_{K\pi}$ flips sign with respect to the SM and it gets smaller in magnitude as s increases. If it is possible to measure $A_{K\pi}$ in a low-energy bin, this would ease the identification of this type of NP in $A_{K\pi}$. When the more realistic limits obtained in Ref. [29] are considered (under the assumption of approximate lepton universality), it is impossible to identify any departures from the SM prediction in this observable. For this reason, we follow Ref. [21] and use

$$\Delta\mathcal{A}_{K\pi} = \mathcal{A}_{K\pi}(s, \hat{\epsilon}_S, \hat{\epsilon}_T) - \mathcal{A}_{K\pi}(s, 0, 0), \quad (5.10)$$

instead. The corresponding (unmeasurably small) deviations from the SM result are plotted in figure 8.

5.5 Limits on $\hat{\epsilon}_S$ and $\hat{\epsilon}_T$

One of the main purposes in the search for NP using the channel $\tau^- \rightarrow \bar{K}^0 \pi^- \nu_\tau$ is to set bounds on the couplings $\hat{\epsilon}_S$ and $\hat{\epsilon}_T$, which are the effective couplings responsible of NP effects in this case. For this task we compare the decay width (Γ) for non-vanishing NP effective couplings with respect to the SM width (Γ^0) where NP is absent. We take the observable Δ defined in the

⁷In eq. (5.9) we use $\mathcal{A}_{K\pi}$ to emphasize the decay channel under consideration and compare it next to our previous result for the $\pi\pi$ decay mode. Otherwise we will also be using the most common notation A_{FB} for this observable.

⁸We note that in this reference, and also later on in Refs. [58, 14], the angle θ used to compute A_{FB} is defined between the three-momenta of the tau lepton and the K_S in the di-meson rest frame. Taking into account the different sign conventions, it can be checked there is reasonable agreement with these works in the elastic region.

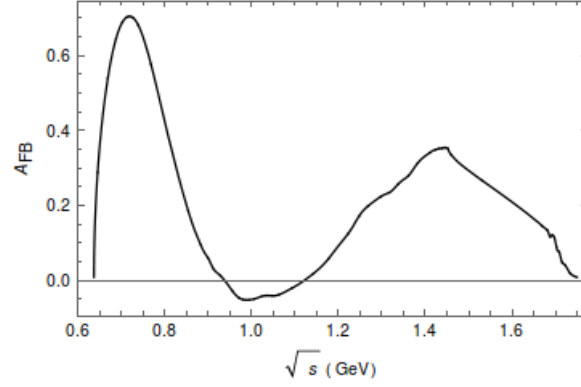


Figure 6: Forward-backward asymmetry in $\tau^- \rightarrow K_S \pi^- \nu_\tau$ decays for the SM case.

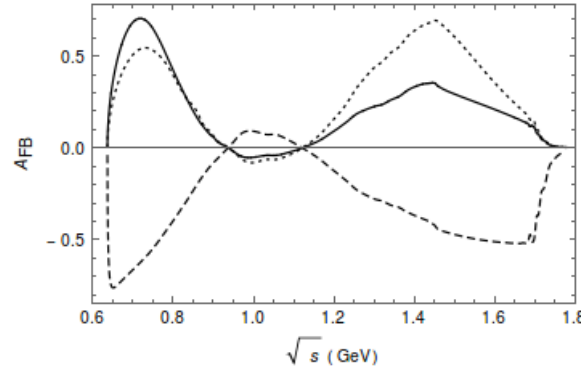


Figure 7: Forward-backward asymmetry in $\tau^- \rightarrow K_S \pi^- \nu_\tau$ decays compared with the SM prediction (solid line). The dashed line corresponds to $\hat{e}_S = -0.5$, $\hat{e}_T = 0$, and the dotted line corresponds to $\hat{e}_S = 0$, $\hat{e}_T = 0.6$.

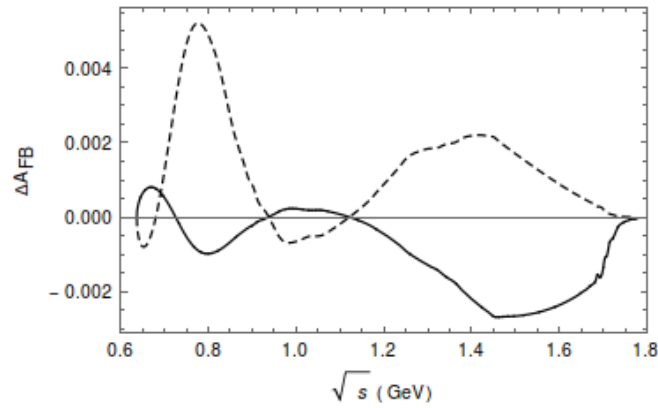


Figure 8: Deviations from the SM forward-backward asymmetry, $\Delta \mathcal{A}_{K\pi}$, in $\tau^- \rightarrow K_S \pi^- \nu_\tau$ decays using the bounds from Ref. [29]. The solid line corresponds to $\hat{e}_S = -8 \times 10^{-4}$, $\hat{e}_T = 0$ and the dashed line to $\hat{e}_S = 0$, $\hat{e}_T = 6 \times 10^{-3}$.

following equation as the appropriate one to enhance the sensitivity to non-vanishing values of $\hat{\epsilon}_S$ and $\hat{\epsilon}_T$.

$$\Delta \equiv \frac{\Gamma - \Gamma^0}{\Gamma^0} = \alpha \hat{\epsilon}_S + \beta \hat{\epsilon}_T + \gamma \hat{\epsilon}_S^2 + \delta \hat{\epsilon}_T^2, \quad (5.11)$$

where we obtained the following results for the coefficients: $\alpha \in [0.30, 0.34]$, $\beta \in [-2.92, -2.35]$, $\gamma \in [0.95, 1.13]$ and $\delta \in [3.57, 5.45]$. The values for $\hat{\epsilon}_S$ and $\hat{\epsilon}_T$ are calculated from eq. (5.11) in two different ways, as it is done in Refs. [20, 21]. First we set one of the couplings to zero obtaining bounds for the other, these results are shown in figure 9.

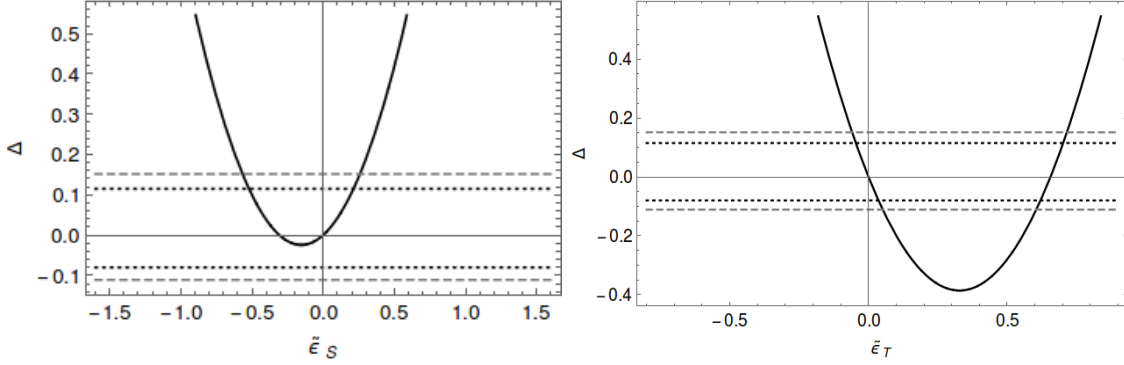


Figure 9: Δ as a function of $\hat{\epsilon}_S$ for $\hat{\epsilon}_T = 0$ (left hand) and of $\hat{\epsilon}_T$ for $\hat{\epsilon}_S = 0$ (right hand) for $\tau^- \rightarrow K_S \pi^- \nu_\tau$ decays. Horizontal lines represent the values of Δ according to the current measurement and theory errors (at three standard deviations) of the branching ratio (dashed line) and in the hypothetical case where the measured branching ratio at Belle-II has a three times reduced uncertainty (dotted line).

Then, we also obtained constrains for $\hat{\epsilon}_S$ and $\hat{\epsilon}_T$ in the general case where both are non-vanishing. We show these results in figure 10, where the bounds on both couplings are limited by an ellipse in the $\hat{\epsilon}_S$ - $\hat{\epsilon}_T$ plane.

The information for the couplings obtained here was used in the previous subsections, where we took the values $\hat{\epsilon}_S \sim -0.5$ and $\hat{\epsilon}_T \sim 0.6$ as representative of realistic maximum absolute values of these coefficients when only the branching ratio (and not the decay spectrum) is considered.

Our results for the bounds in the $\hat{\epsilon}_S$ and $\hat{\epsilon}_T$ couplings are summarized in the following table.

Δ limits	$\hat{\epsilon}_S(\hat{\epsilon}_T = 0)$	$\hat{\epsilon}_T(\hat{\epsilon}_S = 0)$	$\hat{\epsilon}_S$	$\hat{\epsilon}_T$
Current bounds	$[-0.57, 0.27]$	$[-0.059, 0.052] \cup [0.60, 0.72]$	$[-0.89, 0.58]$	$[-0.07, 0.72]$
Future bounds	$[-0.52, 0.22]$	$[-0.047, 0.036] \cup [0.62, 0.71]$	$[-0.87, 0.56]$	$[-0.06, 0.71]$

Table 1: Constraints on the scalar and tensor couplings obtained through the limits on the current branching ratio at three standard deviations using the current theory and experimental errors and assuming the latter be reduced to a third ('Future bounds'). This last case should be taken only as illustrative of the improvement that can be achieved thanks to higher-statistics measurements, even in absence of any progress on the theory side. It is clear that the knowledge of $\hat{\epsilon}_{S,T}$ using $\tau^- \rightarrow K_S \pi^- \nu_\tau$ decays data is limited by theory uncertainties.

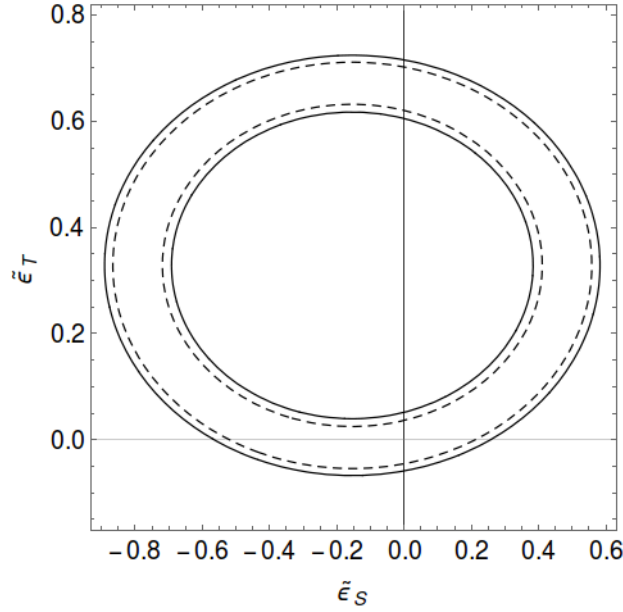


Figure 10: Constraints on the scalar and tensor couplings obtained from $\Delta(\tau^- \rightarrow K_S \pi^- \nu_\tau)$ using theory and the measured value reported in the PDG, with their corresponding uncertainties at three standard deviations (solid line). The dashed line ellipse corresponds to the case where the measurements error was reduced to a third of the current uncertainty.

Next we will consider fits to the branching ratio and decay spectrum⁹ of the $\tau^- \rightarrow K_S \pi^- \nu_\tau$ decays as measured by Belle [9]. We will pay special attention to the possible explanation of the conflicting data points (bins 5, 6 and 7) by the non-standard interactions. Therefore, we will consider fits with and without these data points. In all our fits, as explained e. g. in Ref. [17], we will not consider the first data point (as it lies below the threshold for physical K_S and π^- masses) and will disregard the data from the last 10 bins, as suggested by the Belle collaboration.

The χ^2 function minimized in our fits is

$$\sum_i \left(\frac{\mathcal{N}_i^{exp} - \mathcal{N}_i^{th}}{\sigma_{\mathcal{N}_i}} \right)^2 + \left(\frac{BR^{exp} - BR^{th}}{\sigma_{BR}^{exp}} \right)^2, \quad (5.12)$$

where the sum over the i bins may or may not include the $i = 5, 6, 7$ bins. Our expression for the differential decay rate (5.6) (whose integration yields $BR^{th} \times \Gamma_\tau$) is related to the distribution of the measured number of events as indicated in eq. (3.1) of Ref. [17] and in the subsequent explanation. We will consider the measurement of BR^{exp} reported in the Belle paper [9] (and not the PDG [59] or the HFLAV [60] values), as discussed in Ref. [17]. Along our fits we float the meson form factors within their estimated uncertainty bands and our quoted results take these errors into account.

We summarize our main results in the following table.

⁹P. R. thanks Denis Epifanov for providing him with these data.

Best fit values	$\hat{\epsilon}_S$	$\hat{\epsilon}_T$	χ^2	χ^2 in the SM
Excluding $i = 5, 6, 7$ bins	$(1.3 \pm 0.9) \times 10^{-2}$	$(0.7 \pm 1.0) \times 10^{-2}$	[72, 73]	[74, 77]
Including $i = 5, 6, 7$ bins	$(0.9 \pm 1.0) \times 10^{-2}$	$(1.7 \pm 1.7) \times 10^{-2}$	[83, 86]	[91, 95]

Table 2: Best fit values to the Belle spectrum and branching ratio of the $\tau^- \rightarrow K_S \pi^- \nu_\tau$ decays [9]. The cases where the $i = 5, 6, 7$ bins are excluded/included are considered. We display the reference results obtained floating $\hat{\epsilon}_S$ and $\hat{\epsilon}_T$ simultaneously. In the last two columns the χ^2 of these fits is compared to the SM result.

In view of these results it is clear that the narrow peak structure constituted by the $i = 5, 6, 7$ bins cannot be understood either in the SM (with a dispersive scalar form factor coming from the S-wave of a coupled channels analysis of meson-meson scattering [38]) [18, 10, 11, 12, 13, 15, 14, 16, 17] or in the EFT analysis considered in this work. This conclusion agrees with the later preliminary data of BaBar [62] and a Belle posterior measurement [63], where such a bump near threshold is absent.

Our results $\hat{\epsilon}_S = (1.6 \pm 0.9) \times 10^{-2}$ and $\hat{\epsilon}_T = (0.9 \pm 1.0) \times 10^{-2}$ translate into bounds on the corresponding NP scale $\Lambda \sim 2 - 5$ TeV¹⁰, assuming effective couplings of natural value at $\mu = \Lambda$ and accounting for the running of these coefficients on the renormalization scale μ [61, 25]. These results are, of course, modest compared to the NP reach of (semi)leptonic Kaon decays, which can probe related scales as high as $\mathcal{O}(500)$ TeV [29] for non-standard scalar interactions.

6. CP violation

The observable A_{CP} , measured by BaBar [2] at odds with the SM prediction (tiny corrections from direct CP violation are neglected along this section), is defined as

$$A_{CP} = \frac{\Gamma(\tau^+ \rightarrow \pi^+ K_S \bar{\nu}_\tau) - \Gamma(\tau^- \rightarrow \pi^- K_S \nu_\tau)}{\Gamma(\tau^+ \rightarrow \pi^+ K_S \bar{\nu}_\tau) + \Gamma(\tau^- \rightarrow \pi^- K_S \nu_\tau)}. \quad (6.1)$$

In the SM, A_{CP} is saturated by the neutral kaon mixing contribution. Because of that, it is given by the analogous asymmetry measured in semileptonic kaon decays [8] ($\ell = e, \mu$)

$$\frac{\Gamma(K_L \rightarrow \pi^- \ell^+ \nu_\ell) - \Gamma(K_L \rightarrow \pi^+ \ell^- \bar{\nu}_\ell)}{\Gamma(K_L \rightarrow \pi^- \ell^+ \nu_\ell) + \Gamma(K_L \rightarrow \pi^+ \ell^- \bar{\nu}_\ell)} = 3.32(6) \times 10^{-3}, \quad (6.2)$$

up to small corrections given by the fact that the K_S is reconstructed at the B-factories through its two-prong pion decay mode with a decay time of the order of the K_S lifetime, which modify the previous value to $A_{CP}^{SM} = 3.6(1) \times 10^{-3}$ [64], that is 2.8 σ away from the BaBar measurement, $A_{CP} = -3.6(2.3)(1.1) \times 10^{-3}$.

In Ref. [65] it is shown that -in the presence of beyond the SM (BSM) interactions- A_{CP} is modified to

$$A_{CP} = \frac{A_{CP}^{SM} + A_{CP}^{BSM}}{1 + A_{CP}^{SM} \times A_{CP}^{BSM}}, \quad (6.3)$$

¹⁰Explicitly, $\Lambda \sim v(V_{us}\hat{\epsilon}_{S,T})^{-1/2}$, with $v = (\sqrt{2}G_F)^{-1/2} \sim 246$ GeV.

where, in our case [8]¹¹

$$A_{CP}^{BSM} = \frac{2 \sin \delta_T^W |\hat{\epsilon}_T| G_F^2 |V_{us}|^2 S_{EW}}{256 \pi^3 M_\tau^2 \Gamma(\tau \rightarrow K_S \pi \nu_\tau)} \int_{s_{\pi K}}^{M_\tau^2} ds |f_+(s)| |F_T(s)| \sin(\delta_+(s) - \delta_T(s)) \frac{\lambda^{3/2}(s, m_\pi^2, m_K^2) (M_\tau^2 - s)^2}{s^2}, \quad (6.4)$$

where δ_T^W stands for the relative weak phase between the SM V-A and the tensor contributions. In Ref. [8], using $SU(2)_L$ invariance of the weak interactions and the EFT machinery, poses stringent constraints on $\Im m[\hat{\epsilon}_T]$ by exploiting the measurements of $D - \bar{D}$ mixing and the upper limit on the electric dipole moment of the neutron. This results in the bound $2\Im m[\hat{\epsilon}_T] \lesssim 10^{-5}$, that we will use. To see that δ_T^W is a small parameter, we remind the limits from the global EFT analysis of NP in Kaon (semi)leptonic decays [29], according to which $|\epsilon_T| = (0.5 \pm 5.2) \times 10^{-3}$. Considering this, $\sin \delta_T^W |\hat{\epsilon}_T| \sim \Im m[\hat{\epsilon}_T]$ and the numerical evaluation of eq. (6.4) is straightforward with the inputs at hand.

We have computed eq. (6.4) using $|F_T(s)|$ obtained with $s_{cut} = M_\tau^2, 4, 9 \text{ GeV}^2$ (shown in the left panel of fig. 1) and with $\delta_T(s)$ varying (smoothly) within the band shown in fig. 2 of Ref. [8]. The errors on $|F_+(s)|$ and $\delta_+(s)$ are negligible compared to the uncertainties on $F_T(s)$. Among these two types of uncertainties, the error on $\delta_T(s)$ dominates completely: changing s_{cut} for a given $\delta_T(s)$ can modify A_{CP}^{BSM} by a factor three, at most; while, with a fixed s_{cut} , A_{CP}^{BSM} can be vanishing for $\delta_T(s) \rightarrow \delta_+(s)$ also in the inelastic region. In this way, we find

$$A_{CP}^{BSM} \lesssim 8 \cdot 10^{-7}, \quad (6.5)$$

which is slightly weaker bound than the one reported in Ref. [8]: $A_{CP}^{BSM} \lesssim 3 \cdot 10^{-7}$. This small difference comes from our accounting for the variation in s_{cut} and for the fact that our phase $\delta_+(s)$ has a non-trivial energy-dependence (as shown in the right plot of our fig. 1) as compared to the central curve for $\delta_+(s)$ in Ref. [8], corresponding to a Breit-Wigner approximation for the $K^*(892)$ ¹². In any case, it is clear that heavy BSM interactions can only modify A_{CP} at the 10^{-6} level at most, which is at least three orders of magnitude smaller than the theoretical uncertainty in its prediction (which is, in turn, some 25 times smaller than the error of the BaBar measurement). Therefore, any conclusive anomaly in A_{CP} must be explained outside the framework considered in this paper (and in Ref. [8]); for instance, by BSM effects of very light particles.

7. Conclusions

We arrived at the following three conclusions:

- In agreement with Ref. [8], we confirm that it is not possible to understand within the low-energy limit of the SMEFT framework the BaBar measurement [2] of the CP asymmetry, which disagrees at 2.8σ with the SM prediction [64]. As a consequence of our dedicated treatment of the uncertainties on the tensor form factor, we find a slightly weaker bound than

¹¹We recall that c_T in this reference equals $2\hat{\epsilon}_T$ in our notation.

¹²As a consistency check, we reproduce the bound $A_{CP}^{BSM} \lesssim 3 \cdot 10^{-7}$ [8] using $\delta_+(s)$ corresponding to the middle of the band shown for $\delta_+(s)$ in figure 2 of the quoted reference.

in Ref. [8], $A_{CP}^{BSM} \lesssim 8 \cdot 10^{-7}$, which is anyway some three (five) orders of magnitude smaller than the theoretical uncertainty in its prediction (the error of the BaBar measurement). If the BaBar anomaly is confirmed, its explanation must be due to light NP. A determination of this quantity with Belle-I data, together with the future measurement at Belle-II [56], will shed light on this puzzle.

- The bins number 5, 6 and 7 of the Belle measurement [9] of the $K_S \pi^-$ mass spectrum in $\tau^- \rightarrow K_S \pi^- \nu_\tau$ decays could not find an explanation using a scalar form factor obtained from the corresponding partial-wave of a meson-meson scattering coupled channels analysis [38, 11]¹³. We have shown here, for the first time, that non-standard scalar or tensor interactions produced by heavy NP are not capable of explaining these data points either. Again a caveat remains with respect to light NP effects, which are beyond the scope of this paper.
- Current branching ratio and spectrum measurements of the $\tau^- \rightarrow K_S \pi^- \nu_\tau$ decays restrict the NP effective couplings, ε_S and ε_T , as we have studied in this work for the first time. Our results are consistent with naive expectations: while the considered decays set bounds similar to those coming from hyperon semileptonic decays (which are at the level of a few TeV NP energy scale under reasonable assumptions), they are not competitive with (semi)leptonic Kaon decays, that could probe $\mathcal{O}(500)$ TeV NP generating non-standard scalar interactions. However, we put forward that tensor interactions are probed in $\tau^- \rightarrow (K\pi)^- \nu_\tau$ decays with similar NP energy reach than in (semi)leptonic Kaon and hyperon decays. Therefore, the corresponding comparisons for ε_T are meaningful tests of lepton universality and under this assumption tau decays can complement Kaon and hyperon physics in restricting tensor interactions.

Acknowledgements

I want to thank my advisor Pablo Roig for his support and for the project 250628 (Ciencia Básica) and also conacyt for my PhD scholarship.

References

- [1] J. Rendón, P. Roig and G. Toledo Sánchez, “Effective-field theory analysis of the $\tau^- \rightarrow (K\pi)^- \nu_\tau$ decays,” *Phys. Rev. D* **99**, no. 9, 093005 (2019)
- [2] J. P. Lees *et al.* [BaBar Collaboration], “Search for CP Violation in the Decay $\tau^- \rightarrow \pi^- K_S^0 (>= 0\pi^0) \nu_\tau$,” *Phys. Rev. D* **85** (2012) 031102 Erratum: [*Phys. Rev. D* **85** (2012) 099904].
- [3] M. Kobayashi and T. Maskawa, “CP Violation in the Renormalizable Theory of Weak Interaction,” *Prog. Theor. Phys.* **49** (1973) 652.
- [4] A. D. Sakharov, “Violation of CP Invariance, C asymmetry, and baryon asymmetry of the universe,” *Pisma Zh. Eksp. Teor. Fiz.* **5** (1967) 32 [*JETP Lett.* **5** (1967) 24] [*Sov. Phys. Usp.* **34** (1991) no.5, 392] [*Usp. Fiz. Nauk* **161** (1991) no.5, 61].

¹³The effect of the otherwise dominant vector form factor is kinematically suppressed in this region and can never give such a strong enhancement as observed in these data points.

- [5] A. G. Cohen, D. B. Kaplan and A. E. Nelson, “Progress in electroweak baryogenesis,” *Ann. Rev. Nucl. Part. Sci.* **43** (1993) 27.
- [6] A. Riotto and M. Trodden, “Recent progress in baryogenesis,” *Ann. Rev. Nucl. Part. Sci.* **49** (1999) 35.
- [7] M. Bischofberger *et al.* [Belle Collaboration], “Search for CP violation in $\tau \rightarrow K_S^0 \pi \nu_\tau$ decays at Belle,” *Phys. Rev. Lett.* **107** (2011) 131801.
- [8] V. Cirigliano, A. Crivellin, M. Hoferichter. “No-go theorem for nonstandard explanations of the $\tau \rightarrow K_S \pi \nu_\tau$ CP asymmetry”. *Phys. Rev. Lett.* **120** (2018) no. 44, 141803.
- [9] D. Epifanov *et al.* [Belle Collaboration], “Study of $\tau^- \rightarrow K_S \pi^- \nu_\tau$ decay at Belle,” *Phys. Lett. B* **654** (2007) 65.
- [10] B. Moussallam, “Analyticity constraints on the strangeness changing vector current and applications to $\tau^- \rightarrow K \pi \nu_\tau$, $\tau \rightarrow K \pi \pi \nu_\tau$,” *Eur. Phys. J. C* **53** (2008) 401.
- [11] M. Jamin, A. Pich and J. Portolés, “What can be learned from the Belle spectrum for the decay $\tau^- \rightarrow \nu_\tau K_S \pi^-$,” *Phys. Lett. B* **664** (2008) 78.
- [12] D. R. Boito, R. Escribano and M. Jamin, “K pi vector form-factor, dispersive constraints and $\tau^- \rightarrow \nu_\tau K \pi$ decays,” *Eur. Phys. J. C* **59** (2009) 821.
- [13] D. R. Boito, R. Escribano and M. Jamin, “K π vector form factor constrained by $\tau^- \rightarrow K \pi \nu_\tau$ and K_{l3} decays,” *JHEP* **1009** (2010) 031.
- [14] D. Kimura, K. Y. Lee and T. Morozumi, “The Form factors of $\tau \rightarrow K \pi(\eta) \nu$ and the predictions for CP violation beyond the standard model,” *PTEP* **2013** (2013) 053B03 Erratum: [*PTEP* **2014** (2014) no.8, 089202].
- [15] M. Antonelli, V. Cirigliano, A. Lusiani and E. Passemar. “Predicting the τ strange branching ratios and implications for V_{us} ”. *JHEP* **1310** (2013) 070.
- [16] V. Bernard, “First determination of $f_+(0)|V_{us}|$ from a combined analysis of $\tau \rightarrow K \pi \nu_\tau$ decay and πK scattering with constraints from K_{l3} decays,” *JHEP* **1406** (2014) 082.
- [17] R. Escribano, S. González-Solís, M. Jamin and P. Roig, “Combined analysis of the decays $\tau^- \rightarrow K_S \pi^- \nu_\tau$ and $\tau^- \rightarrow K^- \eta \nu_\tau$,” *JHEP* **1409** (2014) 042.
- [18] M. Jamin, A. Pich and J. Portolés, “Spectral distribution for the decay $\tau^- \rightarrow \nu_\tau K \pi$,” *Phys. Lett. B* **640** (2006) 176.
- [19] L. A. Jiménez Pérez and G. Toledo Sánchez, “Absorptive corrections for vector mesons: matching to complex mass scheme and longitudinal corrections,” *J. Phys. G* **44** (2017) no.12, 125003.
- [20] E. A. Garcés, M. Hernández Villanueva, G. López Castro and P. Roig, “Effective-field theory analysis of the $\tau^- \rightarrow \eta^{(\prime)} \pi^- \nu_\tau$ decays,” *JHEP* **1712** (2017) 027.
- [21] J. A. Miranda and P. Roig, “Effective-field theory analysis of the $\tau^- \rightarrow \pi^- \pi^0 \nu_\tau$ decays”. *JHEP* **1811** (2018) 038.
- [22] V. Cirigliano, A. Falkowski, M. González-Alonso and A. Rodríguez-Sánchez, “Hadronic \tilde{D} Decays as New Physics Probes in the LHC Era,” *Phys. Rev. Lett.* **122**, no. 22, 221801 (2019).
- [23] V. Cirigliano, J. Jenkins and M. González-Alonso, “Semileptonic decays of light quarks beyond the Standard Model,” *Nucl. Phys. B* **830**, 95 (2010).
- [24] T. Bhattacharya, V. Cirigliano, S. D. Cohen, A. Filipuzzi, M. González-Alonso, M. L. Graesser, R. Gupta and H. W. Lin, “Probing Novel Scalar and Tensor Interactions from (Ultra)Cold Neutrons to the LHC,” *Phys. Rev. D* **85**, 054512 (2012).

- [25] V. Cirigliano, M. González-Alonso and M. L. Graesser, “Non-standard Charged Current Interactions: beta decays versus the LHC,” *JHEP* **1302** (2013) 046.
- [26] V. Cirigliano, S. Gardner and B. Holstein, “Beta Decays and Non-Standard Interactions in the LHC Era,” *Prog. Part. Nucl. Phys.* **71** (2013) 93.
- [27] H. M. Chang, M. González-Alonso and J. Martín Camalich, “Nonstandard Semileptonic Hyperon Decays,” *Phys. Rev. Lett.* **114** (2015) no.16, 161802.
- [28] A. Courtoy, S. Baessler, M. González-Alonso and S. Liuti, “Beyond-Standard-Model Tensor Interaction and Hadron Phenomenology,” *Phys. Rev. Lett.* **115** (2015) 162001.
- [29] M. González-Alonso and J. Martín Camalich, “Global Effective-Field-Theory analysis of New-Physics effects in (semi)leptonic kaon decays,” *JHEP* **1612** (2016) 052.
- [30] M. González-Alonso and J. Martín Camalich, “New Physics in $s \rightarrow u\ell^- \bar{\nu}$: Interplay between semileptonic kaon and hyperon decays,” arXiv:1606.06037 [hep-ph].
- [31] S. Alioli, V. Cirigliano, W. Dekens, J. de Vries and E. Mereghetti, “Right-handed charged currents in the era of the Large Hadron Collider,” *JHEP* **1705** (2017) 086.
- [32] M. González-Alonso, J. Martín Camalich and K. Mimouni, “Renormalization-group evolution of new physics contributions to (semi)leptonic meson decays,” *Phys. Lett. B* **772** (2017) 777.
- [33] M. González-Alonso, O. Naviliat-Cuncic and N. Severijns, “New physics searches in nuclear and neutron β decay,” *Prog. Part. Nucl. Phys.* **104** (2019) 165.
- [34] P. Roig, “Semileptonic τ decays: powerful probes of non-standard charged current weak interactions,” *EPJ Web Conf.* **212**, 08002 (2019) [arXiv:1903.02682 [hep-ph]].
- [35] W. Buchmuller and D. Wyler, “Effective Lagrangian Analysis of New Interactions and Flavor Conservation,” *Nucl. Phys. B* **268** (1986) 621.
- [36] B. Grzadkowski, M. Iskrzynski, M. Misiak and J. Rosiek, “Dimension-Six Terms in the Standard Model Lagrangian,” *JHEP* **1010** (2010) 085.
- [37] M. Jamin, J. A. Oller and A. Pich, “Strangeness changing scalar form-factors,” *Nucl. Phys. B* **622** (2002) 279.
- [38] M. Jamin, J. A. Oller and A. Pich, “S wave K pi scattering in chiral perturbation theory with resonances,” *Nucl. Phys. B* **587** (2000) 331.
- [39] J. Gasser and H. Leutwyler, “Chiral Perturbation Theory to One Loop,” *Annals Phys.* **158** (1984) 142.
- [40] J. Gasser and H. Leutwyler, “Chiral Perturbation Theory: Expansions in the Mass of the Strange Quark,” *Nucl. Phys. B* **250** (1985) 465.
- [41] G. Ecker, J. Gasser, A. Pich and E. de Rafael, “The Role of Resonances in Chiral Perturbation Theory,” *Nucl. Phys. B* **321** (1989) 311.
- [42] G. Ecker, J. Gasser, H. Leutwyler, A. Pich and E. de Rafael, “Chiral Lagrangians for Massive Spin 1 Fields,” *Phys. Lett. B* **223** (1989) 425.
- [43] A. Sirlin, “Radiative corrections to $g(\nu)/g(\mu)$ in simple extensions of the $su(2) \times u(1)$ gauge model,” *Nucl. Phys. B* **71** (1974) 29.
- [44] A. Sirlin, “Current Algebra Formulation of Radiative Corrections in Gauge Theories and the Universality of the Weak Interactions,” *Rev. Mod. Phys.* **50** (1978) 573 Erratum: [*Rev. Mod. Phys.* **50** (1978) 905].

- [45] A. Sirlin, “Large $m(W)$, $m(Z)$ Behavior of the $O(\alpha)$ Corrections to Semileptonic Processes Mediated by W ,” Nucl. Phys. B **196** (1982) 83.
- [46] W. J. Marciano and A. Sirlin, “Radiative Corrections to beta Decay and the Possibility of a Fourth Generation,” Phys. Rev. Lett. **56** (1986) 22.
- [47] W. J. Marciano and A. Sirlin, “Electroweak Radiative Corrections to tau Decay,” Phys. Rev. Lett. **61** (1988) 1815.
- [48] W. J. Marciano and A. Sirlin, “Radiative corrections to $\pi(\text{lepton } 2)$ decays,” Phys. Rev. Lett. **71** (1993) 3629.
- [49] E. Braaten and C. S. Li, “Electroweak radiative corrections to the semihadronic decay rate of the tau lepton,” Phys. Rev. D **42** (1990) 3888.
- [50] J. Erler, “Electroweak radiative corrections to semileptonic tau decays,” Rev. Mex. Fis. **50** (2004) 200.
- [51] M. Jamin, J. A. Oller and A. Pich, “Scalar $K\pi$ form factor and light quark masses,” Phys. Rev. D **74**, 074009 (2006).
- [52] O. Cata and V. Mateu, “Chiral perturbation theory with tensor sources,” JHEP **0709**, 078 (2007).
- [53] I. Baum, V. Lubicz, G. Martinelli, L. Orifici and S. Simula, “Matrix elements of the electromagnetic operator between kaon and pion states,” Phys. Rev. D **84**, 074503 (2011).
- [54] S. González-Solís and P. Roig, “A dispersive analysis of the pion vector form factor and $\tau^- \rightarrow K^- K_S \nu_\tau$ decay,” Eur. Phys. J. C **79**, no. 5, 436 (2019)
- [55] P. Buettiker, S. Descotes-Genon and B. Moussallam, “A new analysis of πK scattering from Roy and Steiner type equations,” Eur. Phys. J. C **33** (2004) 409.
- [56] E. Kou *et al.* [Belle II Collaboration], “The Belle II Physics Book,” arXiv:1808.10567 [hep-ex].
- [57] L. Beldjoudi and T. N. Truong, “tau to pi K neutrino decay and pi K scattering,” Phys. Lett. B **351** (1995) 357.
- [58] D. N. Gao and X. F. Wang, “On the angular distributions of $\tau^- \rightarrow K_S \pi^- \nu_\tau$ decay,” Phys. Rev. D **87** (2013) 073016.
- [59] M. Tanabashi *et al.* [Particle Data Group], “Review of Particle Physics,” Phys. Rev. D **98** (2018) no.3, 030001.
- [60] Y. Amhis *et al.* [HFLAV Collaboration], “Averages of b -hadron, c -hadron, and τ -lepton properties as of summer 2016,” Eur. Phys. J. C **77** (2017) no.12, 895.
- [61] D. J. Broadhurst and A. G. Grozin, “Matching QCD and HQET heavy - light currents at two loops and beyond,” Phys. Rev. D **52** (1995) 4082.
- [62] S. Paramesvaran [BaBar Collaboration], “Selected topics in tau physics from BaBar,” arXiv:0910.2884 [hep-ex]. Proceedings of the Meeting of the Division of the American Physical Society, DPF 2009, Detroit, USA, July 26-31, 2009.
- [63] S. Ryu [Belle Collaboration], “Measurement of the branching fractions and mass spectra for τ lepton decays including K_S^0 at Belle,” Nucl. Phys. Proc. Suppl. **253-255** (2014) 33.
- [64] Y. Grossman and Y. Nir, “CP Violation in $\tau \rightarrow \nu \pi K_S$ and $D \rightarrow \pi K_S$: The Importance of $K_S - K_L$ Interference,” JHEP **1204** (2012) 002.
- [65] H. Z. Devi, L. Dhargyal and N. Sinha, “Can the observed CP asymmetry in $\tau \rightarrow K \pi \nu_\tau$ be due to nonstandard tensor interactions?,” Phys. Rev. D **90** (2014) no.1, 013016.